Journal Pre-proof

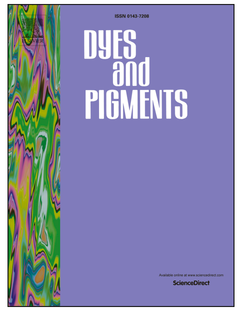

Functionalized coumarin derivatives containing aromatic-imidazole unit as organic luminescent materials

Youjia Wang, Yanmei Li, Tianzhi Yu, Wenming Su, Hailin Ma, Yuling Zhao, Xinyu Li, Hui Zhang

PII: S0143-7208(19)32007-8

DOI: https://doi.org/10.1016/j.dyepig.2019.107958

Reference: DYPI 107958

To appear in: *Dyes and Pigments*

Received Date: 27 August 2019

Revised Date: 7 October 2019

Accepted Date: 7 October 2019

Please cite this article as: Wang Y, Li Y, Yu T, Su W, Ma H, Zhao Y, Li X, Zhang H, Functionalized coumarin derivatives containing aromatic-imidazole unit as organic luminescent materials, *Dyes and Pigments* (2019), doi: https://doi.org/10.1016/j.dyepig.2019.107958.

Graphical Abstract:

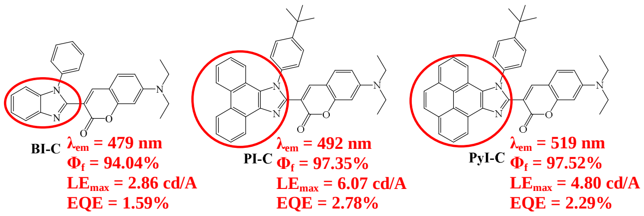

Functionalized Coumarin Derivatives Containing Aromatic-imidazole Unit as Organic Luminescent Materials

Youjia Wang‡[1], Yanmei Li‡[1], Tianzhi Yu[1,*], Wenming Su[2,*], Hailin Ma[1], Yuling Zhao[3], Xinyu Li[1], Hui Zhang[1]

[1]Key Laboratory of Opto-Electronic Technology and Intelligent Control (Ministry of Education), Lanzhou Jiaotong University, Lanzhou 730070, China

[2]Printable electronics research center, Suzhou Institute of Nano-Tech and Nano-Bionics, Chinese Academy of Sciences, Suzhou 215123, China

[3]School of Chemical and Biological Engineering, Lanzhou Jiaotong University, Lanzhou 730070, China

Abstract: Three new coumarin derivatives containing aromatic-imidazole unit (i.e., benzo[*d*]imidazole, phenanthro[9,10-*d*]imidazole and pyreno[4,5-*d*]imidazole), 3-(1-phenyl-1*H*-benzo[d]imidazol-2-yl)-7-(diethylamino)coumarin (**BI-C**), 3-(1-(4-(tert-butyl)phenyl)-1*H*-phenanthro[9,10-*d*]imidazol-2-yl)-7-(diethylamino)coumarin (**PI-C**) and 3-(9-(4-(tert-butyl)phenyl)-9*H*-pyreno[4,5-*d*]imidazol-10-yl)-7-(diethylamino)coumarin (**PyI-C**), were successfully prepared for organic light-emitting devices. These compounds show good thermal properties and strong emissions from greenish-blue to green lights owing to the extended π-conjugation of the rigid polyaromatic imidazole skeleton, and have high photoluminescence quantum efficiency of 94%, 97% and 98% in chloroform solutions. Among these compounds, the doped organic light-emitting device fabricated from the compound **PI-C**

* Corresponding Authors.
Tianzhi Yu, E-mail: yutzh@mail.lzjtu.cn; Wenming Su, E-mail: wmsu2008@sinano.ac.cn
‡These authors are contributed equally

exhibited the maximum luminous efficiency of 6.07 cd/A and maximum EQE of 2.78%.

Key words: Coumarin derivative; Rigid polyaromatic imidazole derivative; Photoluminescence; Electroluminescence

1. Introduction

Coumarin derivatives have attracted attentions owing to the relative ease of synthesis and their outstanding optical properties, which exhibit high fluorescence quantum yields, large Stokes shifts, excellent photostability and thermal stability. Coumarin derivatives have been often used as fluorescent dyes [1], fluorescent probes [2-5], and optical functional materials for organic light-emitting devices (OLEDs) [6-10] and dye-sensitized solar cells [11-14] for decades. Since coumarin 540 (3-(2-benzothiazolyl)-7-diethylaminocoumarin) was firstly used as an efficient organic emitting material in OLEDs [6], and many synthetic coumarin derivatives have successfully been applied in OLEDs [7,8,15-22]. However, the photophysical properties of coumarin derivatives strongly rely upon their molecular structures [23-26]. Coumarin itself shows a very weak blue emission with peak at 430 nm [27], whereas its derivative attached an electron-donating substituent (most commonly an amine group or a hydroxyl group) on 7-position of coumarin skeleton can exhibit strong blue-green emission due to the enhancement of intramolecular charge transfer. In particular, an electron-donating group and an electron-withdrawing group were attached on 7- and 3-position of coumarin ring, respectively, forming a push-pull electron effect, the fluorescent properties of coumarins are greatly enhanced [28]. However, there are the concentration-quenching effect (CQE) or the aggregation-caused quenching (ACQ), coumarin derivatives exhibit usually weak emission, even their fluorescence is quenched in the concentrated solution and solid state. Thus, as emitting materials coumarin derivatives are usually doped in host materials at appropriate concentration to fabricate OLEDs [15-20]. For reducing the self-aggregation quenching of coumarin derivatives at higher concentration or in the solid state, the grafting of the sterically hindered substituents to the coumarin skeleton is an effective method for highly efficient OLEDs [7,21].

The aromatic π–conjugated imidazole moiety is an electron-deficient group, which has been widely employed in the electron-transporting materials and as the electron-withdrawing group of bipolar molecular [29-31]. Recently, the aromatic π–conjugated imidazole moieties have often been used to construct some organic optoelectronic functional materials for OLEDs due to their ambipolar characteristics, high photoluminescence quantum yield, high stability, high triplet energy and pure blue emission [32-38]. In this work, three new coumarin derivatives with D–π–A structure were synthesized by grafting the aromatic π–conjugated imidazole moieties (benzo[*d*]imidazole (BI), phenanthro[9,10-*d*]imidazole (PI) and pyreno[4,5-*d*]imidazole (PyI)) as an electron-withdrawing groups onto the 3-position of coumarin ring and linking diethylamine as an electron-donating group to the 7-position of coumarin ring (Scheme 1). By introducing the different conjugated aromatic imidazole moieties into the coumarin derivatives, we attempt to explore the relationship between the structure and properties of these compounds.

2. Experimental

2.1 Materials and methods

4-(Diethylamino)-2-hydroxybenzaldehyde, 2-aminodiphenylamine, phenanthrene-9,10-dione, pyrene and 4-tert-butylaniline were obtained from Energy Chemical (China). All the other reactants and solvents were obtained from commercial sources.

The preparation of the intermediate pyrene-4,5-dione was described in our previous paper [39].

NMR spectra were measured on Bruker 500, AVANCE NEO. Mass spectra were recorded using a Thermo Scientific Orbitrap Elite mass spectrometer. C, H, and N analyses were obtained using an Elemental Vario-EL automatic elemental analysis instrument. Thermogravimetric analysis (TGA) was performed on a PerkinElmer Pyris system. UV-vis absorption spectra were recorded on a Shimadzu UV-2550 spectrometer. The cyclic voltammograms were performed on a electrochemical analyzer (CHI Instruments 760 B). The photoluminescence quantum yield was measured by an absolute method using the Edinburgh Instruments FLS920 integrating sphere with the Xe lamp at room temperature. The photoluminescence decay lifetime was measured by a time-correlated single photon counting spectrometer using Edinburgh Instruments FLS920 with a microsecond flashlamp as the excitation source (repetition rate 90 Hz) at room temperature.

2.2 Synthesis of the coumarin derivatives

7-Diethylamino-coumarin: Diethyl malonate (5.95 g, 0.037 mol) and 4-(diethylamino)-2-hydroxybenzaldehyde (6.00 g, 0.031 mol) were dissolved in absolute ethyl alcohol (100 ml), and then piperidin (1 mL) was added stepwise under ice bath. Under N_2, the reaction mixture was refluxed at 80 ^{o}C for 6 h. After evaporating solvent in vacuum, 40 mL of concentrated HCl/glacial acetic acid (1:1, v/v) was added into the reaction mixture. The reaction solution was continued to stir for 6 h at 120 ^{o}C. After cooling to room temperature, the resulting mixture was poured into 100 mL of water and neutralized with sodium hydroxide solution (40%) until the pH to 7. The greynish-white precipitate was filtered and recrystallized from toluene to obtain 6.25 g (93%) of 7-diethylamino-coumarin. ^{1}H NMR (500 MHz, $CDCl_3$, δ): 7.51 (d, J = 8.8

Hz, 1H), 7.22 (d, J = 8.4 Hz, 1H), 6.54 (d, J = 8.4 Hz, 1H), 6.46 (s, 1H), 6.01 (d, J = 8.8 Hz, 1H), 3.39 (q, J = 7.1 Hz, 4H), 1.19 (t, J = 7.1 Hz, 6H).

7-(Diethylamino)coumarin-3-carbaldehyde: Under N_2, anhydrous DMF (13.30 mL, 172.5 mmol) was dropped into $POCl_3$ (3.16 ml, 34.5 mmol) with stirring for 6 h in an ice bath. The solution of 7-diethylamino-coumarin (3.00 g, 13.8 mmol) in anhydrous 1,2-dichloroethane was added to the above solution, and the mixture was stirred at 60 ^oC for 12 h. After completing, the mixture was poured into ice water and neutralized with NaOH solution (20%) to pH 7. The formed precipitate was filtered off and washed three times with water. The residue was chromatographed on silica, eluting with petroleum ether/CH_2Cl_2 (2:1, v/v) to form orange solid (2.57 g, 76%). ^{1}HNMR (500 MHz, $CDCl_3$, δ): 10.10 (s, 1H, -CHO), 8.25(s, 1H), 7.41 (d, J = 8.0 Hz, 1H), 6.64 (d, J = 8.0 Hz, 1H), 6.49 (s, 1H), 3.48 (q, J = 8.2 Hz, 4H), 0.96 (t, J = 8.2 Hz, 6H).

BI-C: Under N_2, a mixture of 7-(diethylamino)coumarin-3-carbaldehyde (0.80 g, 3.26 mmol), 2-aminodiphenylamine (0.60 g, 3.26 mmol) and 2-ethoxyethanol (60 mL) was refluxed at 105 ^oC for 12 h. After completing, the reaction mixture was poured into water and extracted with dichloromethane, and the organic phase was dried over anhydrous Na_2SO_4. After removal of solvent, the residue was purified by silica gel column chromatography using ethyl acetate/petroleum ether (1:1, v/v) as eluent. The product as faint yellow solid was obtained (0.81 g, 61%). m.p. > 260 ^oC. ^{1}H NMR (500 MHz, $CDCl_3$, δ): 8.16 (s, 1H), 7.86 (d, J = 8.5 Hz, 1H), 7.47 (t, J = 8.8 Hz, 2H), 7.41-7.37 (m, 3H), 7.34 (t, J = 8.8 Hz, 3H), 7.28 (d, J = 7.5 Hz, 1H), 6.59 (d, J = 8.8 Hz, 1H), 6.42 (s, 1H), 3.42 (q, J = 7.2 Hz, 4H), 1.21 (t, J = 7.2 Hz, 6H). ^{13}C NMR (126 MHz, $CDCl_3$, δ): 159.11, 157.39, 151.49, 149.14, 146.34, 142.72, 136.95, 136.64, 129.85, 129.48, 128.21, 126.35, 123.49, 122.83, 119.76, 111.162, 110.45, 109.18, 108.20, 97.12, 45.01, 29.50.

HRMS: Calcd. for $C_{26}H_{23}N_3O_2$, 410.1863 $[M+H]^+$; Found: 410.1865. Anal. Calcd. for $C_{26}H_{23}N_3O_2$: C, 76.26; H, 5.66; N, 10.26. Found: C, 76.38; H, 5.63; N, 10.30.

PI-C: A mixture of 9,10-Phenanthraquinone (0.90 g, 4.32 mmol), 4-tert-butylaniline (0.80 g, 5.36 mmol), 7-(diethylamino)coumarin-3-carbaldehyde (1.06 g, 4.32 mmol) and NH_4OAc (4.0 g, 51.89 mmol) with 120 mL of AcOH was stirred at 120 ^oC for 12 h under nitrogen atmosphere. After cooling down, the reaction mixture was poured into water and extracted with dichloromethane (3 × 100 mL). The organic phase was washed with water (2 × 100 mL) and dried over anhydrous Na_2SO_4. After removal of solvent, the residue was purified by silica gel column chromatography using ethyl acetate/petroleum ether (1:1, v/v) as eluent to obtain yellow solid (1.21 g, 50%). m.p. > 260 ^oC. ^1H NMR (500 MHz, $CDCl_3$, δ): 8.80 (d, *J* = 8.0 Hz, 1H), 8.75 (d, *J* = 8.4 Hz, 1H), 8.71 (dd, *J* = 8.8 Hz, 2H), 7.94 (s, 1H), 7.74-7.62 (m, 4H), 7.50 (dd, *J* = 8.8 Hz, 3H), 7.15 (d, *J* = 8.5 Hz, 1H), 6.67 (d, *J* = 8.8 Hz, 1H), 6.57 (d, *J* = 8.8 Hz, 1H), 6.43 (s, 1H), 3.42 (q, *J* = 7.2 Hz, 4H), 1.39 (s, 9H), 1.21 (t, *J* = 7.2 Hz, 6H). ^{13}C NMR (126 MHz, $CDCl_3$, δ): 160.16, 157.24, 152.69, 151.34, 147.61, 146.31, 144.32, 137.26, 135.12, 130.39, 129.66, 129.27, 128.44, 128.21, 127.23, 127.20, 126.43, 126.23, 125.44, 124.93, 123.96, 123.66, 123.38, 123.25, 123.10, 122.65, 121.26, 121.01, 111.98, 109.66, 108.96, 108.15, 97.07, 44.87, 34.70, 31.21, 29.80. HRMS: Calcd. for $C_{38}H_{35}N_3O_2$, 566.2802 $[M+H]^+$; Found: 566.2816. Anal. Calcd. for $C_{38}H_{35}N_3O_2$: C, 80.68; H, 6.24; N, 7.43. Found: C, 80.81; H, 6.21; N, 7.46.

PyI-C: The synthetic procedure of the compound **PyI-C** was similar to that of the compound **PI-C**. Yield: 50% (1.35 g). m.p.: > 260 □. ^1H NMR (500 MHz, $CDCl_3$, δ): 9.04 (d, *J* = 7.5 Hz, 1H), 8.17 (d, *J* = 7.5 Hz, 1H), 8.12 (d, *J* = 9.0 Hz, 1H), 8.09 (d, *J* = 8.5 Hz, 1H), 8.03 (m, 3H), 7.64 (t, *J* = 8.0 Hz, 1H), 7.56 (d, *J* = 8.0 Hz, 4H), 7.38 (d, *J* = 7.5 Hz, 1H), 7.29 (d, *J* = 8.8 Hz, 1H), 6.57 (d, J = 8.5 Hz, 1H), 6.44 (s, 1H), 3.41 (q, J = 7.0 Hz, 4H), 1.42 (s, 9H), 1.21 (t, J = 6.5 Hz, 6H). ^{13}C NMR (126 MHz, $CDCl_3$, δ): 160.19, 157.24, 152.77, 151.33, 147.84, 146.40, 137.78, 135.11, 132.07, 131.67, 129.68, 129.10, 128.53, 127.85, 127.53, 126.45, 126.39, 126.31, 125.29, 124.37, 124.31, 123.53, 122.80, 122.42, 119.65, 118.12, 111.90, 108.96, 108.14, 97.03, 44.86, 34.99, 31.23, 12.73. HRMS: Calcd. for $C_{40}H_{35}N_3O_2$, 590.2803 $[M+H]^+$; Found: 590.2778. Anal. Calcd. for $C_{40}H_{35}N_3O_2$: C, 81.47; H, 5.98; N, 7.13. Found: C, 81.26; H, 6.02; N, 7.11.

3. Results and discussion

3.1 Synthesis

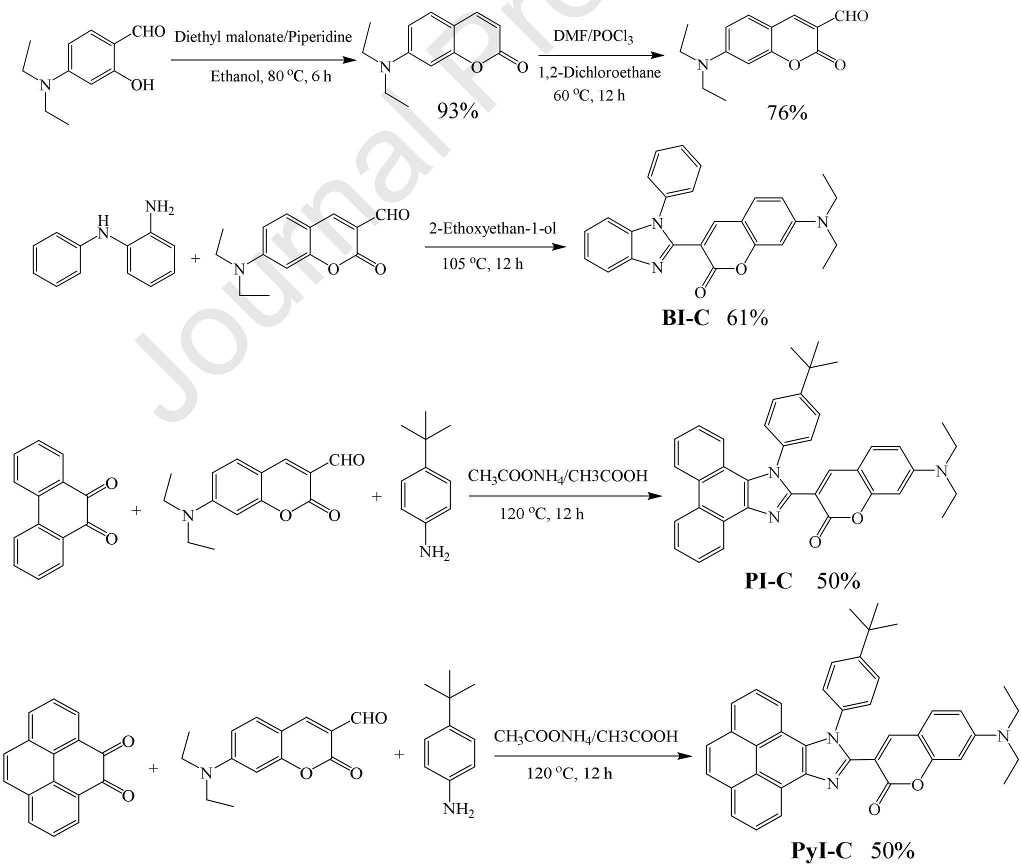

Scheme 1. Synthetic routes to the coumarin derivatives.

The synthetic procedures of the coumarin derivatives (**BI-C**, **PI-C** and **PyI-C**) are illustrated in Scheme 1. The key intermediate, 7-(diethylamino)coumarin-3-carbaldehyde, were obtained through two step reactions from 4-(diethylamino)-2-hydroxybenzaldehyde. First, the intermediate 7-diethylamino-coumarin was prepared from Knoevenagel condensation reaction of 4-(diethylamino)-2-hydroxybenzaldehyde with diethyl malonate, and then the subsequent Vilsmeier-Haack formylation of 7-diethylamino-coumarin in 1,2-dichloroethane produced 7-(diethylamino)coumarin-3-carbaldehyde in 76% yield. The compound **BI-C** was synthesized from 2-aminodiphenylamine and 7-(diethylamino)coumarin-3-carbaldehyde in 2-ethoxyethanol as faint yellow solid with moderate yield (61%) after purification by column chromatography. The compounds **PI-C** and **PyI-C** were synthesized by one-pot multicomponent reaction of the corresponding diketone (phenanthrene-9,10-dione or pyrene-4,5-dione), ammonium acetate and 7-(diethylamino)coumarin-3-carbaldehyde with acetic acid as the medium, and their yields are about 50% after purification by column chromatography. The structures of the compounds were confirmed through ^{1}H, ^{13}C NMR, high resolution mass spectra and elemental analyses. All the compounds have good solubility in common organic solvents, such as THF, dichloromethane, chloroform and toluene. The detailed synthetic procedures and analyses were described in experimental section.

3.2 Thermal stabilities, photophysical and electrochemical properties

The thermal stability of the functional materials is crucial to achieving highly stable device performance. Thus, the thermal properties of **BI-C**, **PI-C** and **PyI-C** were characterized by thermogravimetric analysis (TGA) under a N_2 atmosphere. As shown in Fig. 1, these compounds exhibited excellent thermal stability (> 330 ^{o}C), and the thermal decomposition temperatures (T_d) of the compounds increase gradually with increasing the conjugation degree of the aromatic π–

conjugated imidazole moiety. The thermal decomposition temperatures of **BI-C**, **PI-C** and **PyI-C** are about 343, 384 and 412 ^{o}C at 2% loss of initial weight, respectively, and a sharp weight loss appeared in their TGA curves, indicating that the compounds **BI-C**, **PI-C** and **PyI-C** underwent one large-stage decomposition process.

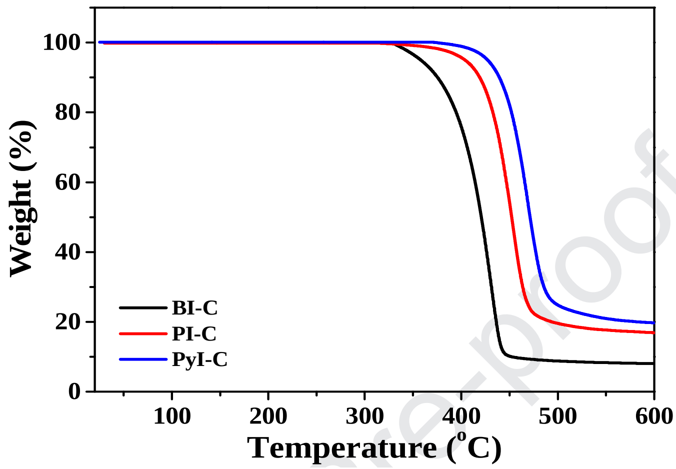

Fig. 1. Thermogravimetric analyses (TGA) of **BI-C**, **PI-C** and **PyI-C** in nitrogen atmosphere (heating rate: 10 °C/min).

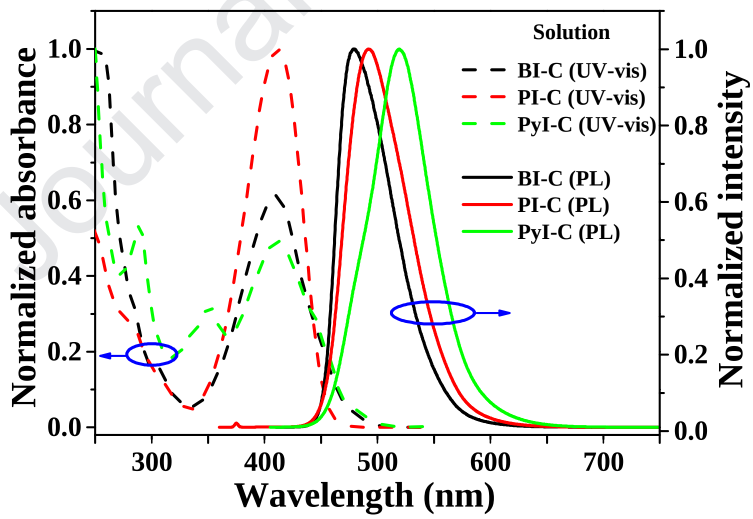

Fig. 2. UV–vis absorption and photoluminescence spectra of the compounds **BI-C**, **PI-C** and **PyI-C** in dichloromethane solutions (C = 1.0×10^{-5} mol/L).

Figure 2 shows the UV-vis absorption and photoluminescence spectra of the compounds **BI-C**, **PI-C** and **PyI-C** at room temperature in CH_2Cl_2 solutions, and the related photophysical data are summarized in Table 1. The compounds **BI-C** and **PI-C** have similarly shaped absorption spectra in the range of 300–550 nm, and the most obvious absorption bands are at 410 nm. This absorption band is assigned to the π–π^* transition of the characteristic vibrational structure of 7-diethylamino-coumarin moiety [17,40]. Besides, there is a very small absorption peak at 289 nm in the absorption spectrum of the compound **PI-C**, which should be assigned to π–π^* transition of phenanthro[9,10-*d*]imidazole (PI) unit. However, the compound **PyI-C** not only exhibits the stronger absorption band at 410 nm, but also two weaker absorption bands at 289 and 351 nm, and the absorption peaks at 289 and 351 nm could be ascribed to π–π^* transition of pyreno[4,5-*d*]imidazole (PyI) unit. From their absorption spectra, the absorption bands of the aromatic π–conjugated imidazole moieties increase gradually increasing the conjugation degree of the aromatic π–conjugated imidazole moiety. Upon excitation at 410 nm, the maximum emission peaks of **BI-C**, **PI-C** and **PyI-C** in CH_2Cl_2 solutions were observed at 479, 492 and 519 nm, respectively. Compared with **BI-C**, the compounds **PI-C** and **PyI-C** exhibit bathochromic shifts of 13 and 40 nm because of increasing conjugation by the aromatic imidazole moieties.

Additionally, the fluorescence quantum yields (Φ_f) of **BI-C**, **PI-C** and **PyI-C** were measured to be 94, 97 and 98% in CH_2Cl_2 solutions at room temperature, respectively, and their fluorescence decay lifetimes (τ) were measured to be 13.2, 12.6 and 12.8 ns. The results show that these compounds have higher Φ_f and belong to the fluorescent emission. Furthermore, we approximately estimated the radiative rate constants (k_r) of **BI-C**, **PI-C** and **PyI-C** to be 7.12×10^7, 7.73×10^7 and 7.62×10^7 s^{-1}, and the nonradiative rate constants (k_{nr}) to be 4.52×10^6, 2.10×10^6 and 1.94×10^6 s^{-1}, respectively, according to the equations: $k_r = \Phi_f/\tau$ and $knr = (1-\Phi_f)/\tau$, assuming that $\Phi_{ISC} = 1$ (ISC = intersystem crossing) [41].

The absorption and photoluminescence (PL) spectra of the compounds in the solid films are similar to those in the solutions, but their absorption and PL spectra in the solid films shift red (Fig. 3). The maximum absorption bands of the compounds in solid films were at 418 nm, which were red-shifted by about 8 nm. The emission peaks of **BI-C**, **PI-C** and **PyI-C** located at 520, 535 and 553 nm, which were red-shifted by 41, 43 and 34 nm, respectively. However, the fluorescence quenching of the compounds is very serious in the solid states, and the fluorescence quantum yields of **BI-C**, **PI-C** and **PyI-C** in the thin films were measured to be 6.5, 14 and 12% at room temperature, respectively.

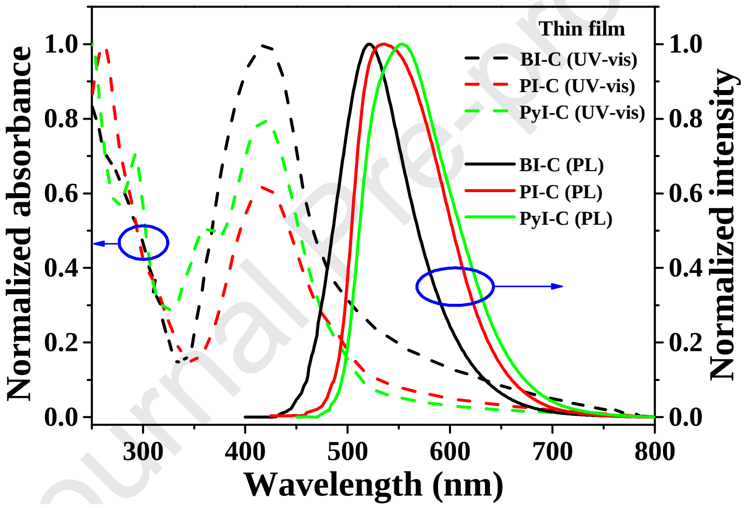

Fig. 3. UV–vis absorption and photoluminescence spectra of the compounds **BI-C**, **PI-C** and **PyI-C** in the solid films.

The electrochemical properties of these compounds were investigated through cyclic voltammetry (CV) at 10 mV/s scan rate in an electrolyte solution of 0.1 M Bu_4NPF_6 dissolved in CH_2Cl_2. Fig. 4 gives the cyclic voltammograms of the compounds **BI-C**, **PI-C** and **PyI-C**. Onset oxidation potentials (E_{onset}) of the compounds are at *ca*. 1.47 V, thus, the HOMO energy levels of the compounds **BI-C**, **PI-C** and **PyI-C** were calculated to be -5.74 eV by the equation [17]: HOMO = -e(Eonset -0.53 + 4.8) eV, in which 0.53 eV was the Fc/Fc^+ potential measured at the same condition. The optical band edges from the absorption spectra of these compounds in CH_2Cl_2

solutions were about 490, 460 and 492 nm for **BI-C**, **PI-C** and **PyI-C**, respectively, which correspond to be 2.53, 2.70 and 2.52 eV from the equation: $E_{opt} = 1241/\lambda_{onset}$. The LUMO energy levels of these compounds are -3.21, -3.04 and -3.22 eV from the equation of LUMO = (HOMO + E_{opt}) eV.

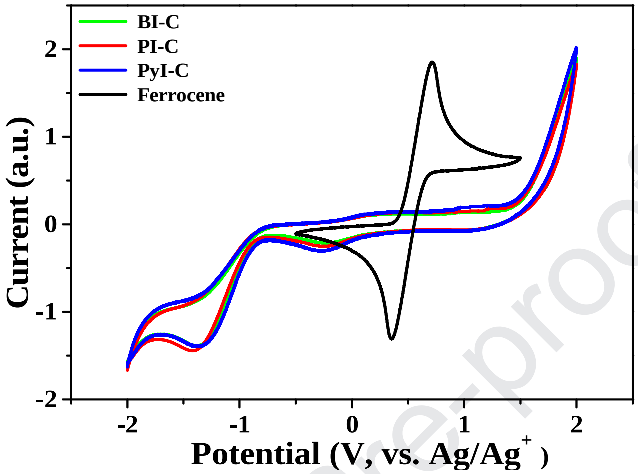

Fig. 4. Cyclic voltammograms of ferrocene and the compounds **BI-C**, **PI-C** and **PyI-C** (scan rate: 10 mV/s; solvent: dichloromethane).

Table 1. Photophysical, thermal and electrochemical properties of the compounds

Compound	UV-vis (nm) (ε (× 10^5 mol^{-1} dm^3 cm^{-1}))	PL (nm)	T_d (°C)	Φ_f (%)	τ (ns)	k_r/k_{nr} (× 10^6 s^{-1})	E_{OX} (V)	E_{opt} (eV)	HOMO/LUMO (eV)
BI-C	410 (3.6)	479	343	94	13.2	71.24/4.52	1.47	2.53	-5.74/-3.21
PI-C	289 (1.6), 410 (5.9)	492	384	97	12.6	77.26/2.10	1.47	2.70	-5.74/-3.04
PyI-C	289 (3.2), 351 (1.8), 410 (2.9)	519	412	98	11.4	76.19/1.94	1.47	2.52	-5.74/-3.22

The structures of the compounds were optimized by density functional theory (DFT) using a B3LYP/6-311G(d) basis set to calculate the frontier molecular orbitals of the compounds. The electronic distributions of the HOMO and LUMO orbitals for the compounds obtained from time-dependent DFT (TD-DFT) calculation are depicted in Fig. 5. In the HOMO orbital of **BI-C**, the electron density completely distributes on the benzoimidazole and 7-(diethylamino)coumarin skeletons, and there is no electron density on the phenyl ring linked to the 2-position of benzoimidazole unit, whereas in its LUMO orbital, most of the electron density resides on the coumarin unit and small part of electron density locates on the benzoimidazole skeleton. For the compounds **PI-C** and **PyI-C**, the electron densities in the HOMO orbitals reside significantly on the phenanthro[9,10-*d*]imidazole or pyreno[4,5-*d*]imidazole skeleton, and small part of electron densities locate on the phenyl ring of (*tert*-butyl)phenyl groups, whereas there are no electron densities on the 7-(diethylamino)coumarin skeletons. The electron density in the LUMO orbital of **PI-C** completely locates on the phenanthro[9,10-*d*]imidazole skeleton, and most of the electron density in the LUMO orbital of **PyI-C** locates on the pyreno[4,5-*d*]imidazole skeleton and very small part of electron densities locate on the phenyl ring of (*tert*-butyl)phenyl group.

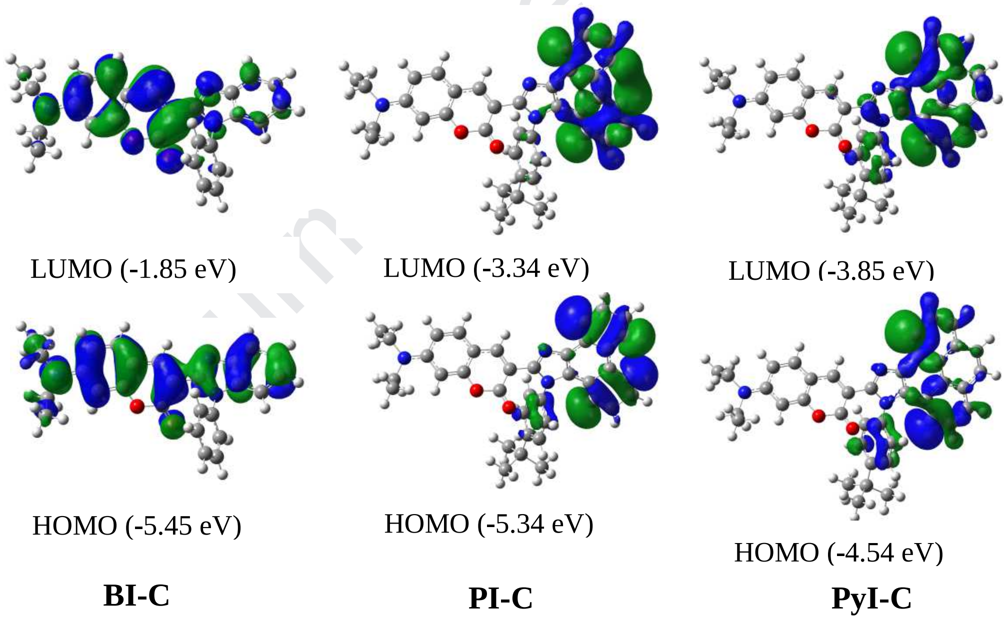

Fig. 5 Frontier orbitals of the compound **A** and **B** calculated at the DFT CAM-B3LYP/6-31+G* level of theory.

3.3 Electroluminescence properties of the compounds

In the light of the excellent thermal stability and strong emission of these compounds in dilute solution, we used these compounds as the emissive materials to fabricate doped OLEDs by vacuum-processed method. The device structures were constructed as: ITO/TAPC (30 nm)/CBP:Dopant (x wt%, 35 nm)/TPBi (30 nm)/Liq (2 nm)/Al (100 nm), in which the codeposited mixture of CBP and the compounds (**BI-C**, **PI-C** and **PyI-C)** was served as the emitting layer, TAPC as the hole-transporting layer, TPBi as the electron transporting and the hole blocking layer, and Liq was used as the electron injection layer. The doped device structure and the energy level diagrams are depicted in Fig. 6.

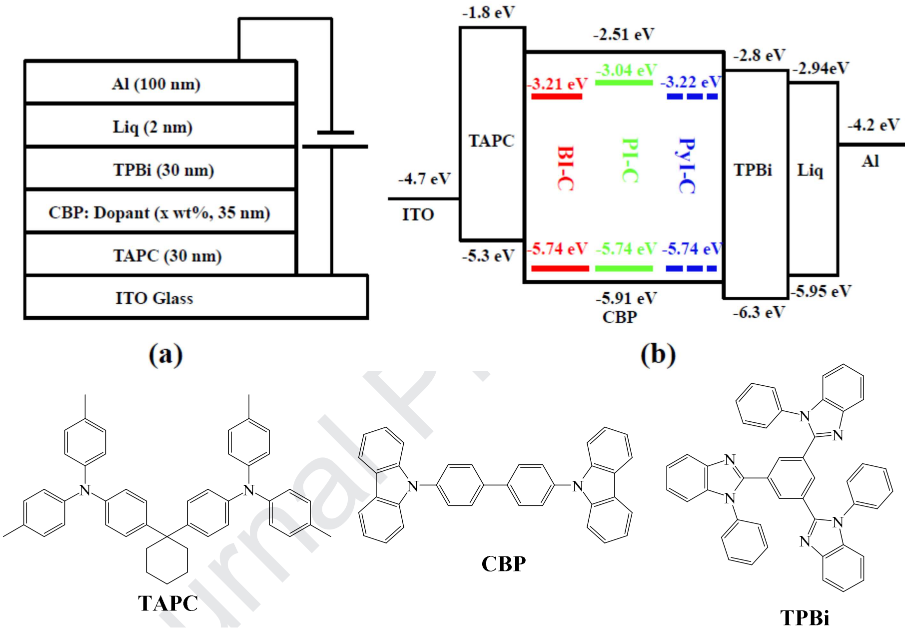

Fig. 6. Schematic diagram of the OLED device configuration (a), the relative HOMO/LUMO energy levels of the materials investigated in this work (b) and structures of TAPC, CBP and TPBi (bottom).

The current density-voltage-luminance (*J–V–L*) characteristics and the EL efficiency curves for these compounds are shown in Fig. 7, Fig. 8 and Fig. 9, and their EL performances are summarized in Table 2. As shown in Fig. 7, at 6 wt% doping concentration of **BI-C**, the device exhibited a maximum current efficiency (CE) of 2.86 cd/A, a power efficiency (PE) of 0.91 lm/W and a maximum external quantum efficiency (EQE) of 1.59%, but a maximum brightness of 1149 cd/m^2 at 12.5 V was observed for the device at 10 wt% doping concentration. As shown in Fig. 8, when the doping concentration of **PI-C** was 12 wt%, the maximum luminance of the fabricated device was 2421 cd/m^2, and the device showed the best EL performance: a maximum CE of 6.07 cd/A, maximum PE of 4.77 lm/W and maximum EQE of 2.78%. From Fig. 9 and Table 2, it is found that the device with 12 wt% doping concentration of **PyI-C** exhibited a maximum luminance of 2598 cd/m^2, maximum CE of 4.80 cd/A, maximum PE of 1.35 lm/W and maximum EQE of 2.29%.

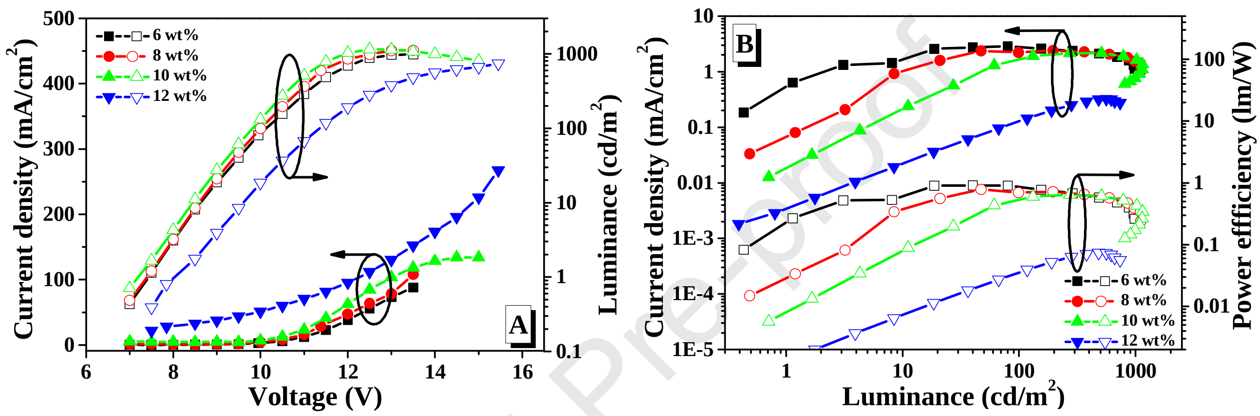

Fig. 7. (A) Luminance-voltage-current density (*L*–*V*–*J*) characteristics and (B) current/power efficiency versus luminance curves of the devices based on **BI-C** with different dopant concentrations.

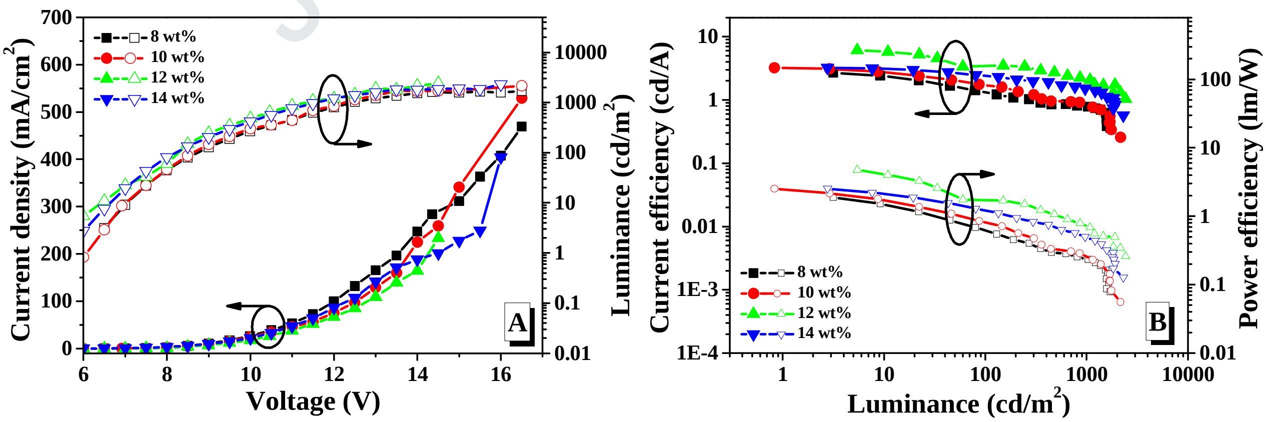

Fig. 8. (A) Luminance-voltage-current density (*L*–*V*–*J*) characteristics and (B) current/power efficiency versus luminance curves of the devices based on **PI-C** with different dopant concentrations.

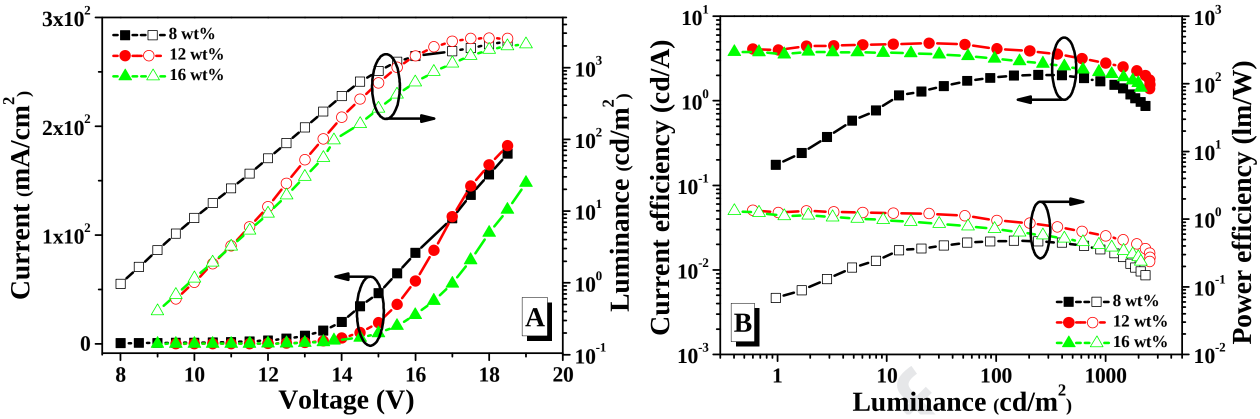

Fig. 9. (A) Luminance-voltage-current density (*L–V–J*) characteristics and (B) current/power efficiency versus luminance curves of the devices based on **PyI-C** with different dopant concentrations.

Table 2. EL performances of the compounds **BI-C**, **PI-C** and **PyI-C**

Compound	Concentration	EL_{max} (nm)	L_{max} (cd/m^2)	LE_{max} (cd/A)	PE_{max} (lm/W)	EQE_{max} (%)
BI-C	6 wt%	479	984	2.86	0.91	1.59
	8 wt%	479	1112	2.39	0.78	1.29
	10 wt%	480	1149	2.15	0.64	1.15
	12 wt%	481	738	0.32	0.07	0.16
PI-C	8 wt%	492	1710	2.42	1.52	2.20
	10 wt%	492	2160	3.23	2.54	2.17
	12 wt%	494	2421	6.07	4.77	2.78
	14 wt%	494	2304	3.17	2.21	2.52
PyI-C	8 wt%	519	2320	2.02	0.48	0.75
	12 wt%	519	2598	4.80	1.35	2.29
	16 wt%	521	2109	3.81	1.32	1.67

Among the three compounds, **PI-C** showed better EL performances than the compounds **BI-C** and **PyI-C**, which is consistent with their radiative rate constants of photoluminescence. Furthermore, the aromatic π–conjugated imidazole groups have bipolar characteristics, which can be used as either electron-acceptor group or electron-donor group [34,35,42,43]. Especially, phenanthroimidazole (PI) shows electron-donating properties when a nature or an electron-withdrawing group is attached to the 2-position of the imidazole ring, but it exhibits electron-withdrawing properties when linked with an electron donor. The order of conjugated degree of the aromatic π–conjugated imidazole groups involved in this paper is as follows: PyI > PI >BI. Compared with PI, BI moiety is more likely to be used as the electron-acceptor [43,44], and PyI unit may prefer to be as electron-donor. Thus, the devices based on the compound **PI-C** may have better carrier balance, which makes the device performance better. In addition, 4-tert-butylphenyl group substituted phenyl group was attached to the 1-position of the imidazole ring in the compounds **PI-C** and **PyI-C**, so the steric hindrance of the compounds **PI-C** and **PyI-C** is greater than that of the compound **BI-C**, suggesting that the intermolecular interaction of **PI-C** or **PyI-C** is smaller than that of **BI-C**. Therefore, the fluorescence quantum yield (Φ_f) and the device performance of the compound **BI-C** are lower than those of the compounds **PI-C** and **PyI-C**.

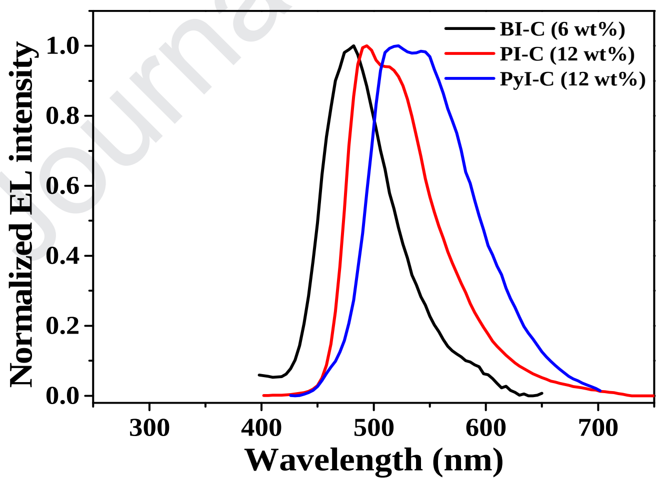

Fig. 10. EL spectra of the devices based on the compounds with maximum luminous efficiencies.

Under the applied voltages, the devices fabricated from these compounds exhibited bright blue-green to green emission with emission peaks at around 479–521 nm (Fig. 10). The electroluminescence (EL) peaks of these compounds are basically consistent with their photoluminescence (PL) peaks in solutions, indicating that the EL originated from their corresponding emitting layer and the charge recombination occurs in the emitting layer. However, in the EL spectra of **PI-C** and **PyI-C**, there is a shoulder peak at longer wavelength resulting from the excimer and exciplex species formed at the interfaces, which also contributed to the emission.

4. Conclusions

Three aromatic-imidazole-based coumarin derivatives (**BI-C**, **PI-C** and **PyI-C**) were designed and prepared for OLEDs, in which the aromatic π–conjugated imidazole moieties (benzo[*d*]imidazole (BI), phenanthro[9,10-*d*]imidazole (PI) and pyreno[4,5-*d*]imidazole (PyI)) as electron-withdrawing groups were grafted onto the 3-position of 7-(diethylamino)coumarin. These compounds exhibited strong blue-green or green emissions with high Φ_f in CH_2Cl_2 solutions as well as good thermal stability (T_d > 340 °C). Among these compounds, the compound **PI-C** showed better PL and EL properties. The fabricated devices based on **PI-C** exhibited the best EL performance with the maximum luminance of 2421 cd/m^2, maximum CE of 6.07 cd/A and maximum EQE of 2.78%.

Acknowledgements

This work was supported by the National Natural Science Foundation of China (Grant 51563014). We also thank to the Instrument Analysis Center of Lanzhou Jiaotong University.

References

[1] Jones G II, Jackson WR, Choi C, Bergmark WR, Solvent effects on emission yield and lifetime

for coumarin laser dyes. Requirements for a rotatory decay mechanism, J. Phys. Chem., 1985, 89, 294–300.

[2] Li HQ, Cai L, Li JX, Hu YX, Zhou PP, Zhang JM, Novel coumarin fluorescent dyes: Synthesis, structural characterization and recognition behavior towards Cu(II) and Ni(II), Dyes and Pigments, 2011, 91, 309–316.

[3] Wagner BD, The use of coumarins as environmentally-sensitive fluorescent probes of heterogeneous inclusion systems, Molecules, 2009, 14, 210–237.

[4] Guha S, Lohar S, Sahana A, Banerjee A, Safin DA, Babashkina MG, Mitoraj MP, Bolte M, Garcia Y, Mukhopadhyay SK, Das D, A coumarin-based “turn-on” fluorescent sensor for the determination of Al^{3+}: single crystal X-ray structure and cell staining properties, Dalton Trans., 2013, 42, 10198–10207.

[5] Cao DX, Liu ZQ, Verwilst P, Koo S, Jangjili P, Kim JS, Lin WY, Coumarin-based small-molecule fluorescent chemosensors, Chem. Rev., 2019, 119, 10403−10519.

[6] Tang CW, VanSlyke SA, Chen CH, Electroluminescence of doped organic thin films, J. Appl. Phys., 1989, 65, 3610–3616.

[7] Chen CT, Chiang CL, Lin YC, Chan LH, Huang CH, Tsai ZW, Chen CT, Ortho-substituent effect on fluorescence and electroluminescence of arylamino-substituted coumarin and stilbene, Org. Lett., 2003, 5, 1261–1264.

[8] Lee MT, Yen CK, Yang WP, Chen HH, Liao CH, Tsai CH, Efficient green coumarin dopants for organic light-emitting devices, Org. Lett., 2004, 6, 1241–1244.

[9] Genco A, Ridolfo A, Savasta S, Patanè S, Gigli G, Mazzeo M, Bright polariton coumarin-based OLEDs operating in the ultrastrong coupling regime, Adv. Optical Mater.,

2018, 1800364.

[10] Yan LQ, Li RJ, Shen W, Qi ZJ, Multiple-color AIE coumarin-based Schiff bases and potential application in yellow OLEDs, J. Lumin., 2018, 194, 151–155.

[11] Feng HJ, Li RR, Song YC, Li XY, Liu B, Novel D-π-A-π-A coumarin dyes for highly efficient dye-sensitized solar cells: Effect of π-bridge on optical, electrochemical, and photovoltaic performance, J. Power Sources, 2017, 345, 59–66.

[12] Liu B, Wang R, Mi WJ, Li XY, Yu HT, Novel branched coumarin dyes for dye-sensitized solar cells: significant improvement in photovoltaic performance by simple structure modification, J. Mater. Chem., 2012, 22, 15379–15387.

[13] Seo KD, Choi IT, Park YG, Kang S, Lee JY, Kim HK, Novel D-A-π-A coumarin dyes containing low band-gap chromophores for dye-sensitised solar cells, Dyes and Pigments, 2012, 94, 469–474.

[14] Jadhava MM, Vaghasiya JV, Patil DS, Soni SS, Sekar N, Structure efficiency relationship in newly synthesized 4-substituted donor-π-acceptor coumarins for dye sensitized solar cells, New J. Chem., 2018, 42, 5267–5275.

[15] Swanson SA, Wallraff GM, Chen JP, Zhang WJ, Bozano LD, Carter KR, Salem JR, Villa R, Scott JC, Stable and efficient fluorescent red and green dyes for external and internal conversion of blue OLED emission, Chem. Mater., 2003, 15, 2305–2312.

[16] Kumar S, Puttaraju B, Patil S, A deep-blue electroluminescent device based on a coumarin derivative, ChemPlusChem, 2016, 81, 384–390.

[17] Yu TZ, Zhu ZY, Bao YJ, Zhao YL, Liu XX, Zhang H, Investigation of novel carbazole-functionalized coumarin derivatives as organic luminescent materials, Dyes and

Pigments, 2017, 147, 260–269.

[18] Yu TZ, Zhang P, Zhao YL, Zhang H, Meng J, Fan DW, Synthesis, characterization and high-efficiency blue electroluminescence based on coumarin derivatives of 7-diethylamino-coumarin-3-carboxamide, Org. Electron., 2009, 10, 653–60.

[19] Yu TZ, Zhang P, Zhao YL, Zhang H, Meng J, Fan DW, Che, LL, Qiu YQ, Synthesis, crystal structure and photo- and electro-luminescence of the coumarin derivatives with benzotriazole moiety, Org. Electron., 2010, 11, 41–9.

[20] Zhang H, Yu TZ, Zhao YL, Fan DW, Xia YJ, Zhang P, Synthesis, crystal structure, photo- and electro-luminescence of 3-(4-(anthracen-10-yl)phenyl)-7-(N,N'-diethylamino) coumarin, Synth. Met., 2010, 160, 1642–1647.

[21] Prachumrak N, Pojanasopa S, Tarsang R, Namuangruk S, Jungsuttiwong S, Keawin T, Sudyoadsuk T, Promarak V, Synthesis and characterization of carbazole dendronized coumarin derivatives as solution-processed non-doped emitters and hole-transporters for electroluminescent devices, New J. Chem., 2014, 38, 3282–3294.

[22] Kumar S, Puttaraju B, Patil S, A deep-blue electroluminescent device based on a coumarin derivative, ChemPlusChem, 2016, 81, 384–390.

[23] Chen CT, Chiang CL, Lin YC, Chan LH, Huang CH, Tsai ZW, Chen CT, Ortho-substituent effect on fluorescence and electroluminescence of arylamino-substituted coumarin and stilbene, Org. Lett., 2003, 5, 1261–1264.

[24] Yee DJ, Balsanek V, Sames D, New tools for molecular imaging of redox metabolism: Development of a fluorogenic probe for 3α-hydroxysteroid dehydrogenases, J. Am. Chem. Soc., 2004, 126, 2282–2283.

[25] Ammar H, Abid S, Fery-Forgues S, Synthesis and spectroscopic study of new biscoumarin dyes based on 7-(4-methylcoumarinyl) diesters, Dyes and Pigments, 2008, 78, 1–7.

[26] Liu XG, Cole JM, Waddell PG, Lin TC, Radia J, Zeidler A, Molecular origins of optoelectronic properties in coumarin dyes: Toward designer solar cell and laser applications, J. Phys. Chem. A, 2012, 116, 727–737.

[27] Yu TZ, Zhao YL, Fan DW, Synthesis, crystal structure and photoluminescence of 3-(1-benzotrizole)-4-methyl-coumarin, J. Mol. Struct., 2006, 791, 18–22.

[28] Li HQ, Cai L, Chen Z (2012). Coumarin-Derived Fluorescent Chemosensors. In: Wang W (ed.) Advances in Chemical Sensors. InTech. pp121–150.

[29] Takizawa S-y, Montes VA, Anzenbacher P, Phenylbenzimidazole-Based New Bipolar Host Materials for Efficient Phosphorescent Organic Light-Emitting Diodes, Chem. Mater., 2009, 21, 2452−2458.

[30] Wang ZM, Lu P, Chen SM, Gao Z, Shen FZ, Zhang WS, Xu YX, Kwok HS, Ma YG, Phenanthro[9,10-*d*]imidazole as a new building block for blue light emitting materials, J. Mater. Chem., 2011, 21 , 5451−5456.

[31] Chen Y-M, Hung W-Y, You H-W, Chaskar A, Ting H-C, Chen H-F, Wong K-T, Liu Y-H, Carbazole–benzimidazole hybrid bipolar host materials for highly efficient green and blue phosphorescent OLEDs, J. Mater. Chem., 2011, 21, 14971−14978.

[32] Liu YL, Bai Q, Li JY, Zhang ST, Zhang C, Lu F, Yang B, Lu P, Efficient pyrene-imidazole derivatives for organic light-emitting diodes, RSC Adv., 2016, 6, 17239−17245.

[33] Kwon J E, Park S, Park SY, Realizing molecular pixel system for full-color fluorescence reproduction: RGB-emitting molecular mixture free from energy transfer crosstalk, J. Am.

Chem. Soc., 2013, 135, 11239−11246.

[34] Gao Z, Liu YL, Wang ZM, Shen FZ, Liu H, Sun GN, Yao L, Lv Y, Lu P, Ma YG, High-efficiency violet-light-emitting materials based on phenanthro[9,10-*d*]imidazole, Chem. Eur. J., 2013, 19, 2602–2605.

[35] Zhang Y, Lai S-L, Tong Q-X, Lo M-F, Ng T-W, Chan M-Y, Wen Z-C, He J, Jeff K-S, Tang X-L, Liu W-M, Ko C-C, Wang P-F, Lee C-S, High efficiency nondoped deep-blue organic light emitting devices based on imidazole-π-triphenylamine derivatives, Chem. Mater., 2012, 24, 61–70.

[36] Chou H-H, Chen Y-H, Hsu H-P, Chang W-H, Chen Y-H, Cheng C-H, Synthesis of diimidazolylstilbenes as n-type blue fluorophores: Alternative dopant materials for highly efficient electroluminescent devices, Adv. Mater., 2012, 24, 5867–5871.

[37] Chen X, Zhuang X-M, Wang Z-Y, Zhu J-J, Tang S-S, Zheng X-H, Liu Y, Tong Q-X, A multifunctional bipolar host material based on phenanthroimidazole for efficient green and red PhOLEDs with low turn-on voltage, Org. Electron., 2019, 69, 85–91.

[38] Shi JJ, Xu L, Chen C, Lv XH, Ding Q, Li WZ, Xue SF, Yang WJ, Efficient and color-purity blue electroluminescence by manipulating the coupling forms of D-A hybrids with phenothiazine as the strong donor, Dyes and Pigments, 2019, 160, 962–970.

[39] Li YM, Li XY, Yu TZ, Su WM, Wang YJ, Zhao YL, Zhang H, Preparation and luminescence properties of isoquinoline-nucleated polycyclic aromatics, Dyes and Pigments, 2020, 172, 107803.

[40] Li YM, Yu TZ, Su WM, Wang YJ, Zhao YL, Zhang H, Polycyclic aromatic hydrocarbon-bridged coumarin derivatives for organic light-emitting devices, Arabian J.

Chem., (2019) https://doi.org/10.1016/j.arabjc.2019.05.006.

[41] Hao ZR, Li M, Liu YJ, Wang YF, Xie GH, Liu Y, Near-infrared emission of dinuclear iridium complexes with hole/electron transporting bridging and their monomer in solutionprocessed organic light-emitting diodes, Dyes and Pigments, 2018, 149, 315–322.

[42] Islam A, Usman K, Wattoo AG, Shahid T, Abbas N, Hafiz Muhammad Adeel Sharif HMA, Siddique AH, Ahmed M, Ge ZY, Ouyang XH, Meta-substituted bipolar imidazole based emitter for efficient non-doped deep blue organic light emitting devices with a high electroluminescence, J. Photochem. Photobiol. A: Chem., 2019, 379, 72–78.

[43] Yuan Y, Chen J-X, Lu F, Tong Q-X, Yang Q-D, Mo H-W, Ng T-W, Wong F-L, Guo Z-Q, Ye J, Chen Z, Zhang X-H, Lee C-S, Bipolar phenanthroimidazole derivatives containing bulky polyaromatic hydrocarbons for nondoped blue electroluminescence devices with high efficiency and low efficiency roll-off, Chem. Mater., 2013, 25, 4957−4965.

[44] Liu B, Zhu Z-L, Zhao J-W, He D, Wang Z-Y, Luo C-Y, Tong, Q-X, Lee C-S, Tao S-L, Ternary acceptor-donor-acceptor asymmetrical phenanthroimidazole molecule for highly efficient near-ultraviolet electroluminescence with external quantum efficiency (EQE) > 4%, Chem. Eur. J., 2018, 24, 15566−15571.

Research Highlights

1. Three aromatic-imidazole-based coumarin derivatives were synthesized for OLEDs.
2. They exhibited strong blue-green or green emissions with high photoluminescence quantum yields in dichloromethane solutions.
3. The devices based on **PI-C** exhibited the brightness of 2421 cd/m^2 and luminous efficiencies of 6.07 cd/A, and EQE of 2.78%.

Electronic Supplementary Information

Functionalized CoumarinDerivatives Containing Aromatic-imidazole Unit as Organic Luminescent Materials

Youjia Wang‡[1], Yanmei Li‡[1],Tianzhi Yu[1,*],Wenming Su[2,*], Hailin Ma[1], Yuling Zhao[3], Xinyu Li[1],Hui Zhang[1]

[1]Key Laboratory of Opto-Electronic Technology and Intelligent Control (Ministry of Education), Lanzhou Jiaotong University, Lanzhou 730070, China

[2]Printable electronics research center, Suzhou Institute of Nano-Tech and Nano-Bionics, Chinese Academy of Sciences, Suzhou 215123, China

[3]School of Chemical and Biological Engineering, Lanzhou Jiaotong University, Lanzhou 730070, China

[*]Corresponding Authors.
Tianzhi Yu, E-mail: yutzh@mail.lzjtu.cn; Wenming Su, E-mail: wmsu2008@sinano.ac.cn
‡These authors are contributed equally

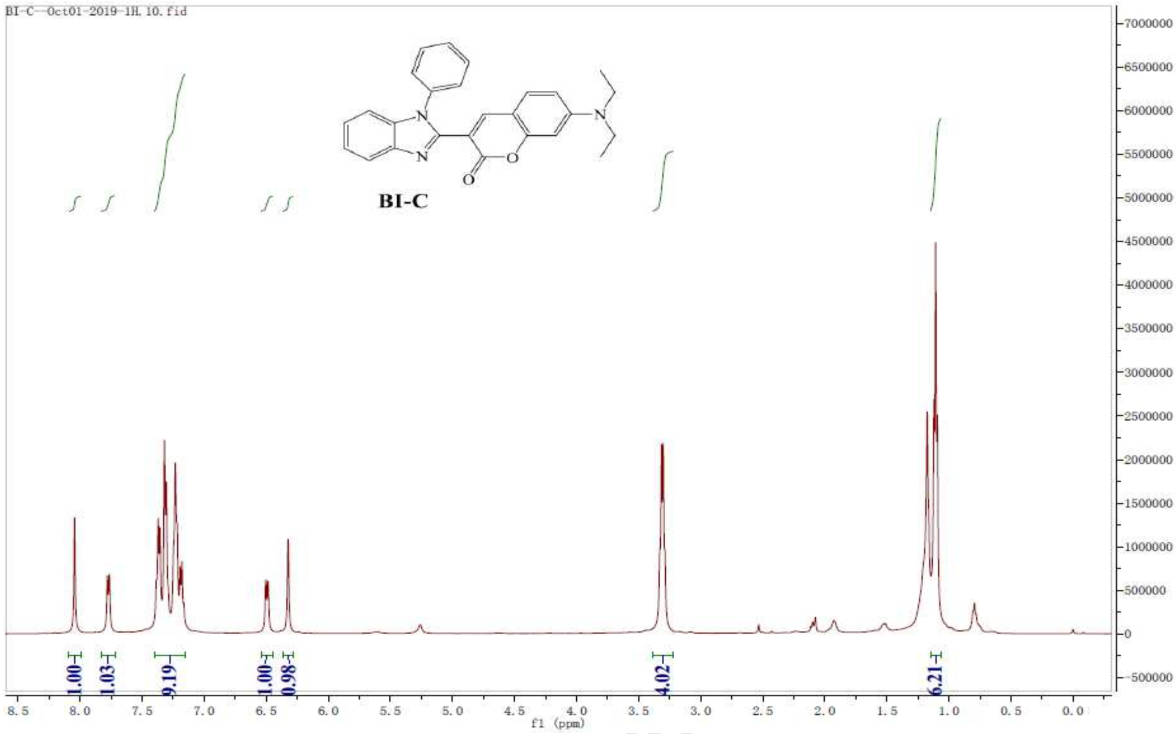

Fig. S1. ^{1}H NMR spectrumof BI-C

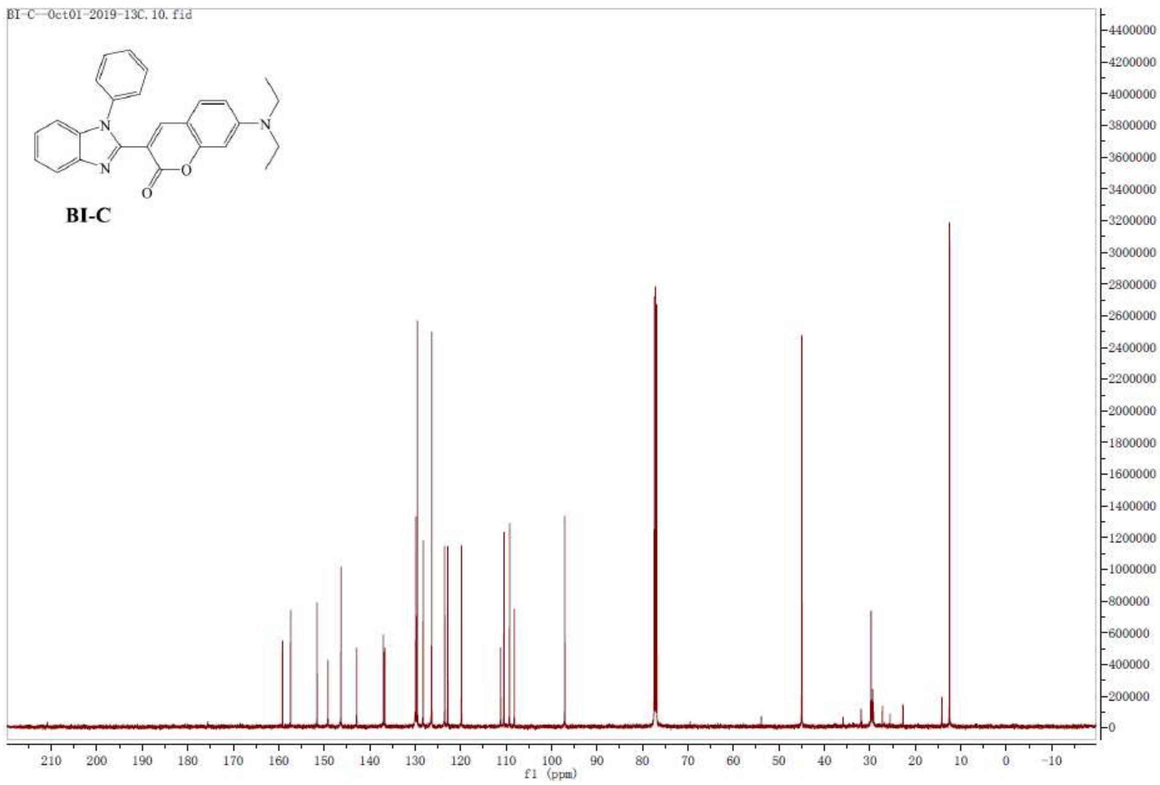

Fig. S2. ^{13}C NMR spectrumof BI-C

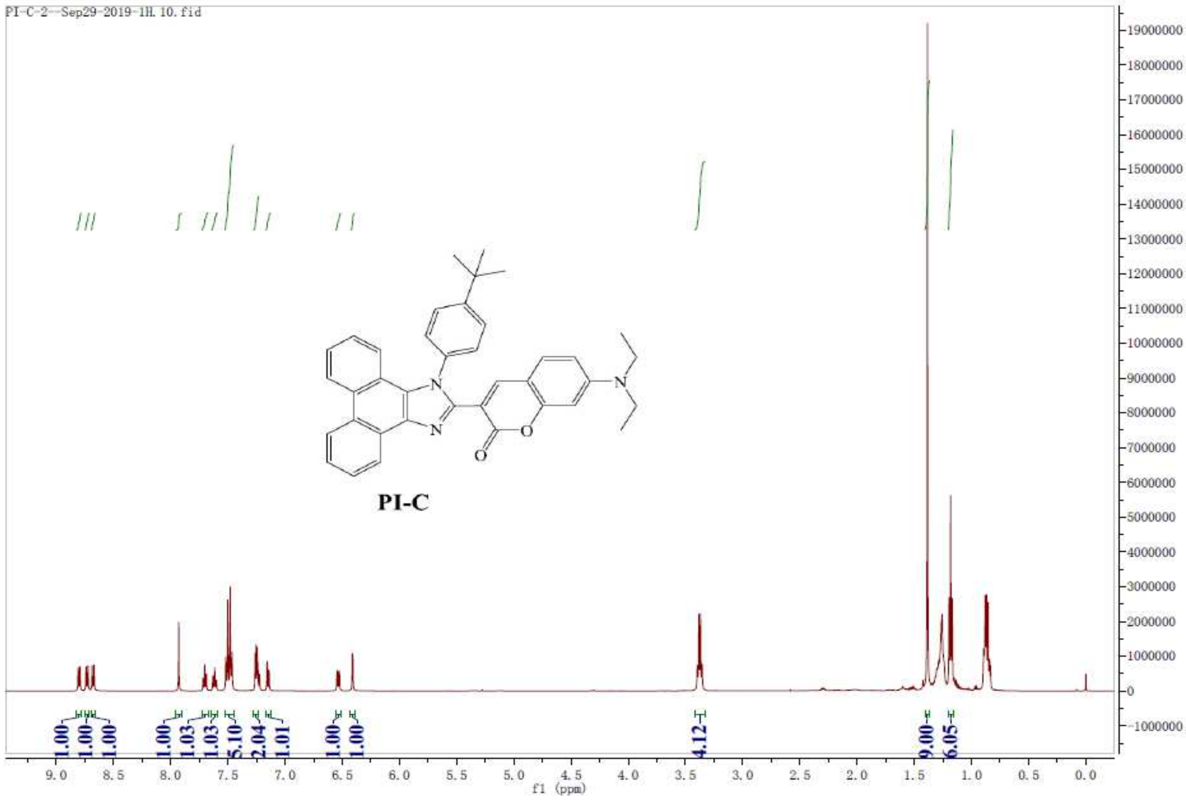

Fig. S3. [1]H NMR spectrumof PI-C

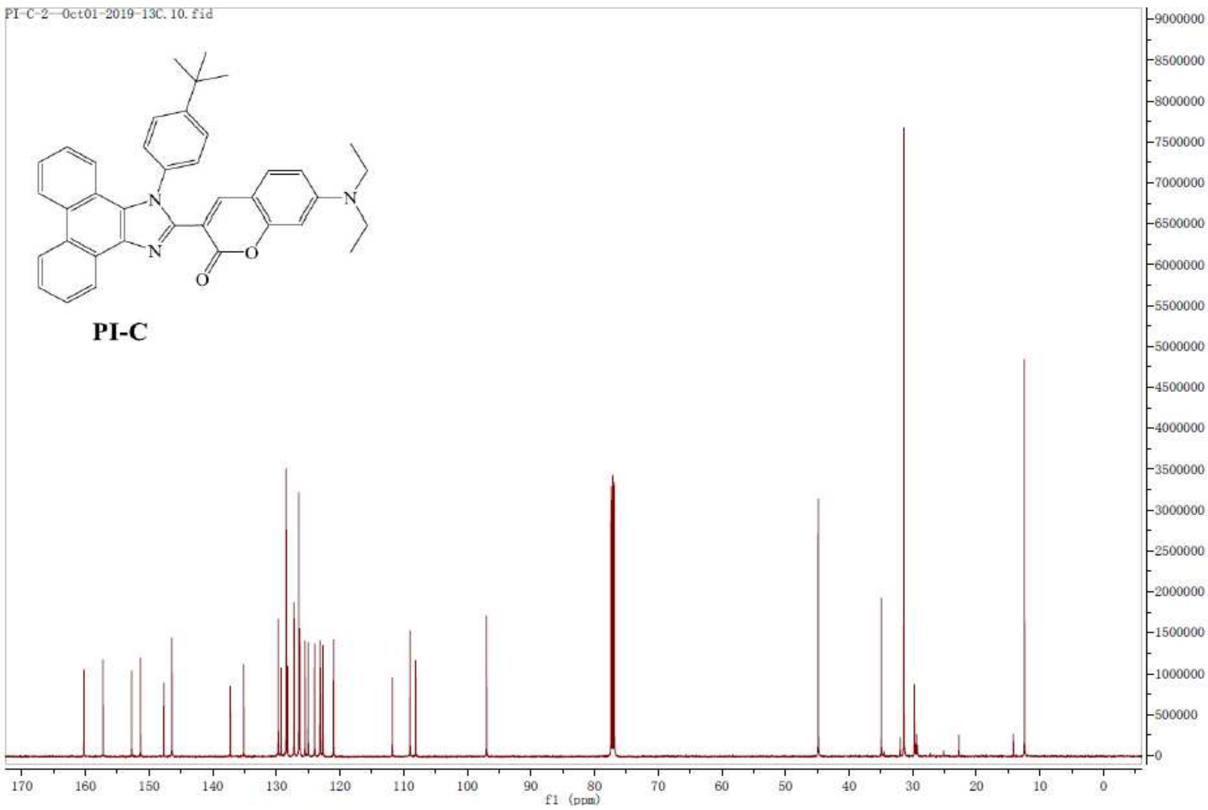

Fig. S4. [13]C NMR spectrumof PI-C

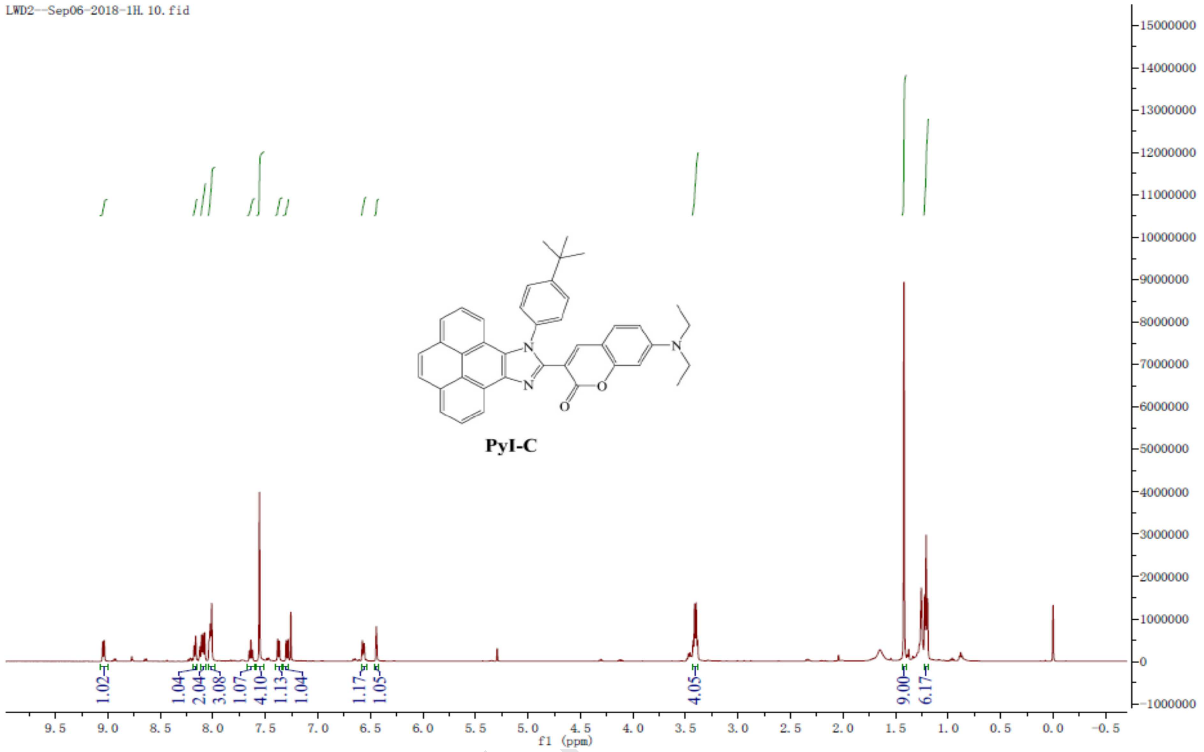

Fig. S5. ^{1}H NMR spectrumofPyI-C

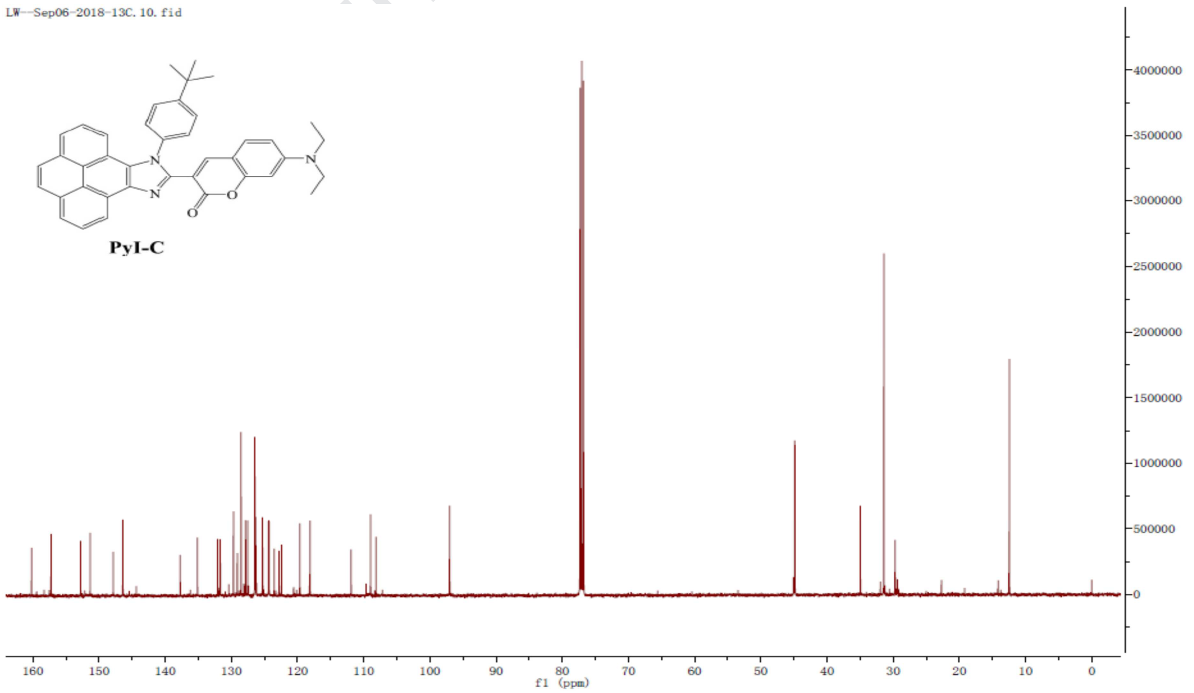

Fig. S6. ^{13}C NMR spectrumofPyI-C

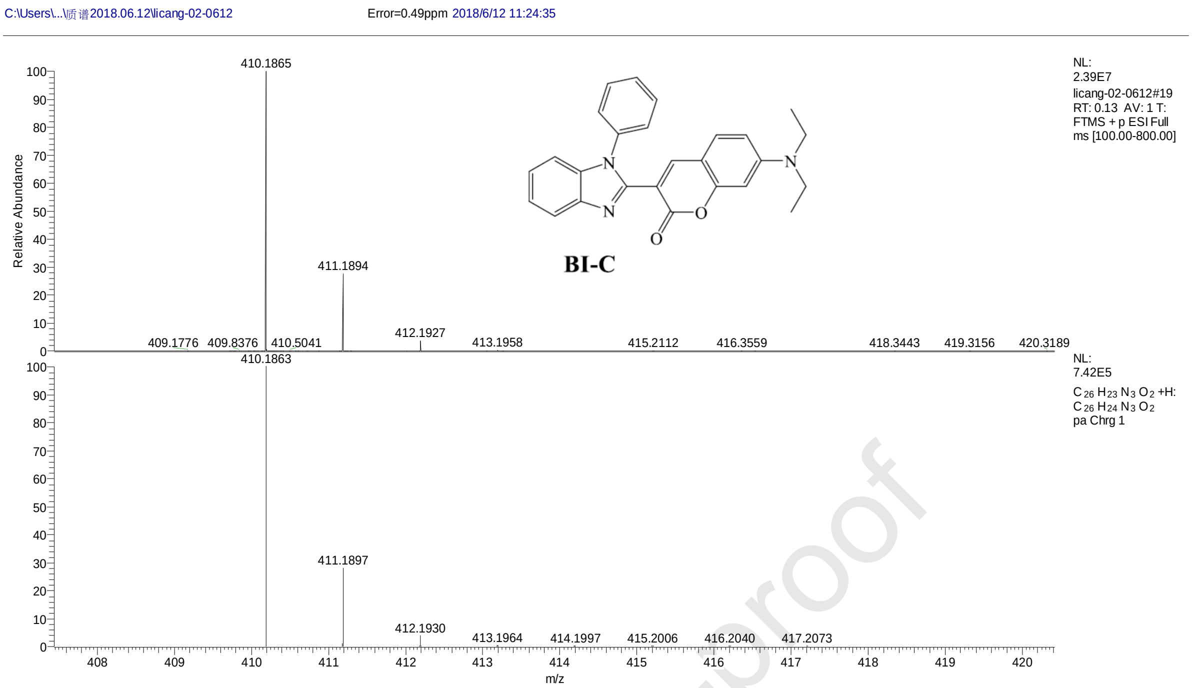

Fig. S7. Mass spectrum of BI-C

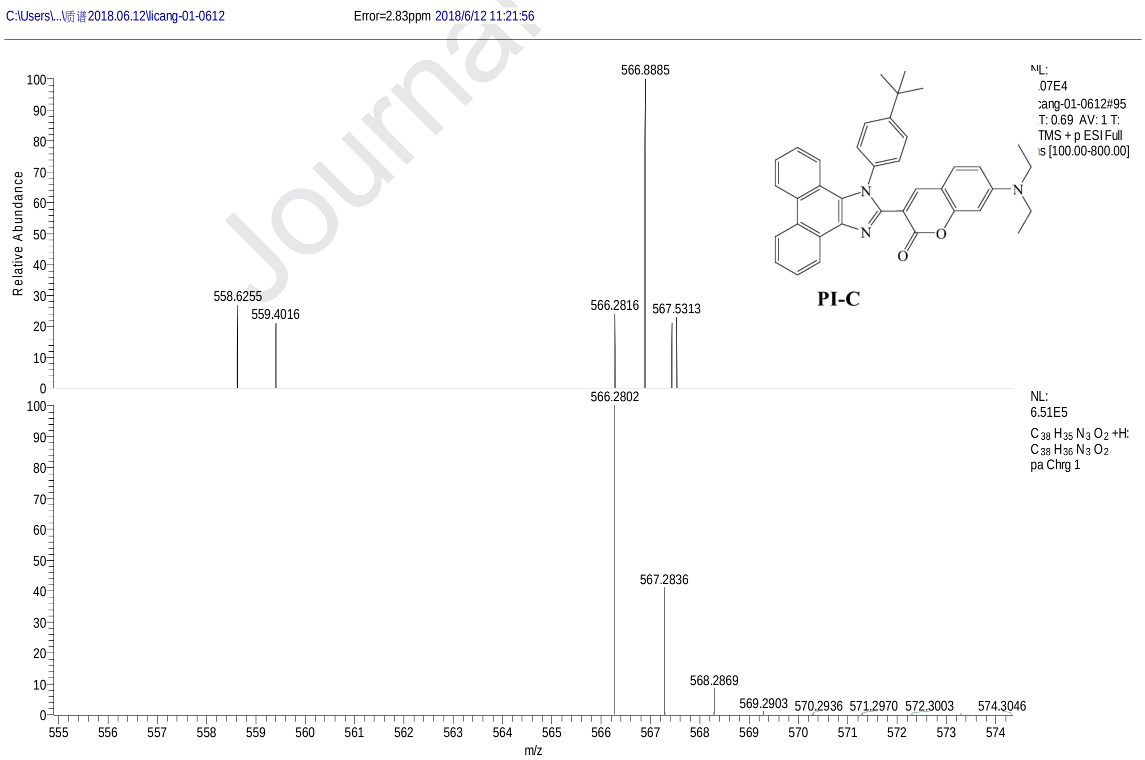

Fig. S8. Mass spectrum of PI-C

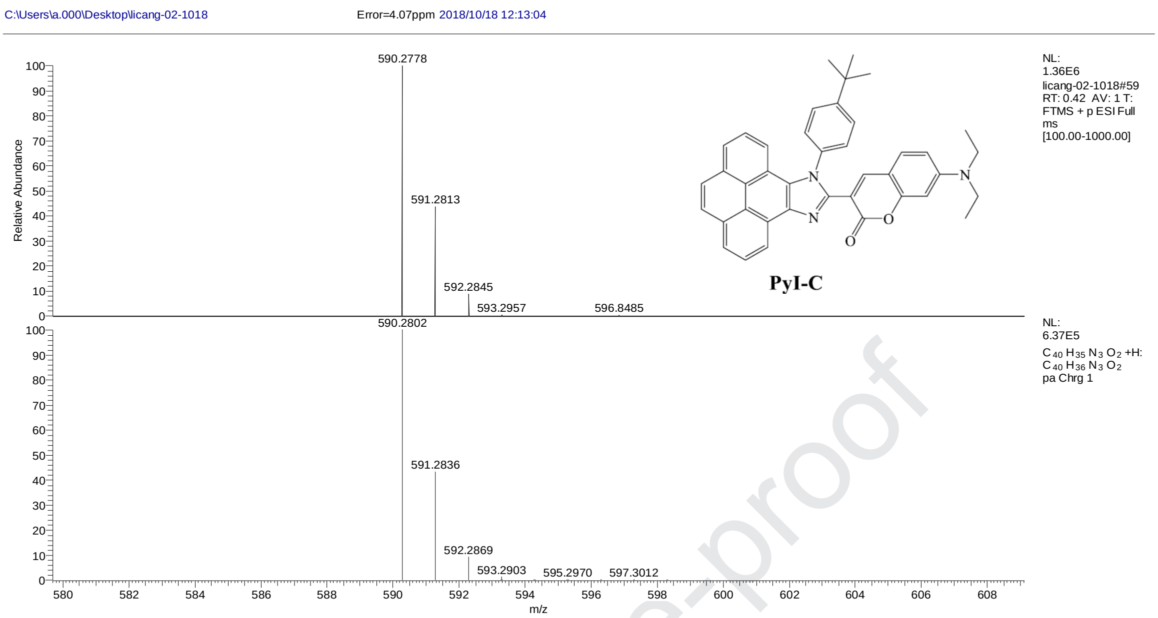

Fig. S9. Mass spectrum ofPyI-C

Dear Sir,

There are no conflicts of interest in this article.

Yours Sincerely

Tianzhi Yu